Density functional study of the conformations and intramolecular proton transfer in thiohydroxamic acids†

Rita Kakkar,* Amita Dua and Sheza Zaidi

Received 28th July 2006, Accepted 27th November 2006
First published as an Advance Article on the web 13th December 2006
DOI: 10.1039/b610899g

The conformational preferences of thiohydroxamic acids (*N*-hydroxythioamides) are investigated by the density functional B3LYP/6-311++G(3df,3pd)//B3LYP/6-31G(d) method in this work. Unlike hydroxamic acids, the thione and thiol forms are found to be equally stable in the gas phase, and the reaction pathways for the interconversion between the thione and thiol forms have been deduced to involve rotation about the C=N bond of the thiol tautomer in the rate-determining step. The effect of aqueous solvation on the reactions has also been investigated. It is found that inclusion of a few explicit water molecules in an implicit solvent calculation is necessary in order to accurately account for hydrogen bonding effects. Thiohydroxamic acids, like their hydroxamic acid analogues, are found to be *N*-acids, both in the gas phase and in aqueous solution.

Introduction

Thiohydroxamic acids [RC(=S)NR′OH] (*N*-hydroxythioamides), like their hydroxamic acid counterparts, play important roles in analytical and biological chemistry.[1] This interesting class of compounds contains a four-atom unit with the diverse atoms C_{sp^2}, S, N and O. The presence of three electronegative atoms, S, N and O, ensures that they have interesting properties. For example, they can act as powerful bidentate ligands, utilizing the S and O atoms, and have found applications in the analytical determination of several metal ions.[2,3] They are also used in nature for the transport of many metal ions.[3] *O*-acyl derivatives of thiohydroxamic acids are efficient precursors of C, S, N, or P radicals.[1,4]

This class of compounds is ubiquitous in nature, being found in diverse sources. *N*-Methyl-*N*-thioformylohydroxylamine, or *N*-methyl thioformohydroxamic acid (R′ = Me), customarily called thioformin, is a bioligand that plays an important role in Fe(III) ion transport through the cell membrane to cells of algae, fungi and bacteria.[5] This function is usually carried out by hydroxamic acids, and thioformin appears to be the only thiohydroxamic acid siderophore discovered so far. *Pseudomonas fluorescens* produces two antibiotics: fluopsin C and fluopsin F,[6–8] which are complexes of Cu(II) and Fe(III), respectively. These antibiotics exhibit high biological activity in relation to both Gram-positive and Gram-negative bacteria. Although SAR studies[9,10] were performed on a number of thioformin derivatives with different R′ groups, none of these has found practical applications because of their toxicity.

Like the corresponding hydroxamic acids, thiohydroxamic acids may exist in the two tautomeric forms: **1**, thione (*N*-hydroxythioamide) or **2**, thiol (*N*-hydroxythioimide). The latter are usually referred to as thiohydroximic acids.

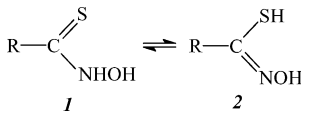

1 *2*

Although solid state[11] and NMR studies reveal that the equilibrium is dominated towards the left, derivatives of **2** are much more common in nature. Sulfated *S*-glucosyl thiohydroximates are biosynthesized by plants belonging to various families, *e.g.* Cruciferae (mustard), nasturtium, *etc.*, and are present in vegetables like cabbage, cauliflower and brussels sprouts.

Many thiohydroxamic and thiohydroximic acids have found applications as biocidal compounds in relation to bacteria, mites, fungi, insects and weeds. They have also been used as antiperspirants and antihypertensive agents, as inhibitors of enzymes, and as drugs for treatment of leukaemia. Thiohydroxamic acids have also been used to counteract the effect of war toxins and to alleviate paralysis.

In spite of these uses, very little is known about their structure, and few computational studies have been reported.[12,13] In view of the biological and other importance of this class of compounds, we have made a systematic study of thiohydroxamic acids. For hydroxamic acids, our previous work[14] had indicated that the calculated relative stabilities are dependent on the basis set chosen for the study. Thus, differences of the order of 2 kcal mol^{-1} for the tautomers, and much larger differences in the case of anion relative energies, were detected from a relative study of basis size dependence, although the energy difference is relatively insensitive to the geometry. Even the order of stabilities is not correctly calculated at the 6-31G(d) level, reinforcing the belief that polarization and diffuse functions are to be compulsorily included, particularly in the case of anion studies.

Herein, we first report the results of a systematic study of the structure of *N*-hydroxythioformamide (thioformohydroxamic acid). We have also determined the relative acidities and stable configurations and tautomers of neutral and deprotonated *N*-thioformamide. It was then substituted at the carbon and nitrogen

Department of Chemistry, University of Delhi, Delhi, 110 007, India. E-mail: rita_kakkar@vsnl.com

† Electronic supplementary information (ESI) available: Optimized Cartesian coordinates, structures, energies and vibrational frequencies. See DOI: 10.1039/b610899g

atoms, respectively, by a methyl group to determine the effect of methyl substitution at these positions.

Computational details

We first carried out calculations on the relative stabilities of the various tautomeric forms of *N*-hydroxythioformamide, and then studied the reaction paths leading from one to the other. Calculations were then repeated for its aqueous solution to see the effect of solvent on the relative stabilities and rotational barriers. Similar calculations were performed for the thioformohydroxamate anion to decide whether thioformohydroxamic acid is an *N*-acid or an *O*-acid.

The DFT calculations were performed with the B3LYP three-parameter density functional, which includes Becke's gradient exchange correction[15] and the Lee–Yang–Parr correlation functional.[16,17] The geometries of all conformers, products and transition states were fully optimized at the B3LYP/6-31G(d) level of theory. This was followed by harmonic frequency calculations at this level. Single-point calculations were then performed at the B3LYP/6-311++G(3df,3pd) level for the geometries optimized at the B3LYP/6-31G(d) level. The SCF = Tight option was used in these calculations, performed using Gaussian 03 Revision B.5.[18] The calculated B3LYP/6-31G(d) vibrational frequencies were used to confirm the nature of all stationary point structures and to account for the zero-point vibrational energy contribution, which was scaled[19] by a factor of 0.9806; the vibrational frequencies were scaled by a factor of 0.9614. The NBO method[20] was used to identify the best Lewis structure representations of the thione and thiol tautomers.

Aqueous phase calculations

The influence of solvation on the relative stability of conformers was studied at two levels: firstly with discrete water molecules, and secondly by examining the effect of bulk solvent using a continuum model. For the first type of calculations, the starting positions of water molecules were carefully selected. First, the desired tautomer was placed in a periodic cubic box of side 18.7 Å, containing 216 TIP3P[21] water molecules. Using a QM/MM method, with the substrate treated quantum mechanically using the PM3 Hamiltonian,[22] and the solvent molecules using the AMBER force field[23] with PM3 charges, the box was equilibrated, applying periodic boundary conditions. A relatively short molecular dynamics simulation (10 ps) of the solvent molecules using the AMBER force field was performed. After a geometry optimization, all water molecules within 5 Å of the substrate molecule were retained, and a geometry optimization again performed. In all cases, it was found that only three such water molecules remained hydrogen-bonded to the tautomer in question. These calculations were performed using the Hyperchem 6.0 software suite.[24]

The influence of bulk solvent was studied by the polarized continuum model (PCM),[25] with the dielectric constant (ε) taken as 78.39 for water at 298.15 K. PCM incorporates electrostatic, dispersion and repulsion contributions to the molecular free energy and cavitation energy. The geometries were fully optimized with respect to the energy with the 6-31G(d) basis set, and single point calculations for the relative energies were performed with the 6-311++G(3df,3pd) basis set.

Results and discussion

Detailed geometrical parameters, vibrational frequencies, energies, and other data are available as electronic supplementary information.†

Besides the thione (**1**) and thiol (**2**) forms, a charge-separated form **3** is also possible:.[13]

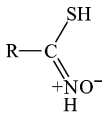

3

Rotation about the double bond is possible in **2**, giving rise to the *Z* and *E* forms:

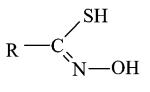

2Z

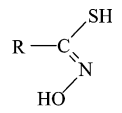

2E

Besides these two structures, different orientations of the S–H and O–H bonds lead to four rotamers for each.

In **1**, too, it is expected that delocalization in the –C(=S)–N– system causes double bond character in the C–N bond system. In this case, too, there are different orientations of the O–H hydrogen:

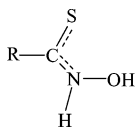

1Z

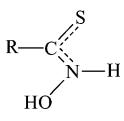

1E

N-Hydroxythioformamide

Relative energies. In Table 1, we report the calculated relative energies of the various structures. Some of the possible structures did not converge, and only the relative energies of the ones that did converge are given in the table. Most of the structures were found to be planar, except **1*E***, in which the mutual repulsion of the O–H and C–H protons causes the structure to become nonplanar. Starting with a planar initial geometry, a structure for **1*E*** was obtained that possesses an imaginary vibrational frequency (471 cm^{-1}), corresponding to out-of-plane movement of nitrogen. Further optimization, allowing the nitrogen to move out of plane, led to a structure having all-real vibrational frequencies, in which the nitrogen adopts a pyramidal orientation. The thiol forms (**2**) are expected to be planar because of the C=N double bond. The planar structure of **1*Z*** points towards conjugative effects that give double bond character to the C–N bond.

In the text, the nomenclature **1*Z***, **1*E***, **2*Z***, **2*E*** and **3** is used to denote the most stable rotamer of each tautomer, *i.e.*, **1*Z*c**, **1*E*t**, **2*Z*tc**, **2*E*tc**, and **3tc**, respectively. The relative energies follow the order **2*Z*** ≈ **1*Z*** < **2*E*** < **1*E*** < **3**. This order agrees with that obtained at the MP2/6-31++G**//MP2/6-31 + G** level,[13] although the difference in energies between **2*Z*** and **1*Z*** reported in the latter calculations is much higher. This can be traced to the smaller value (0.921) that was used by them[13] for scaling the zero-point energies. The calculated relative stability order favours the *Z* forms over the *E* forms. This is in contrast to the situation

Table 1 B3LYP/6-311++G(3df,3pd)//B3LYP/6-31G(d) gas-phase relative energies and aqueous solution relative free energies of the various stationary points on the gas phase *N*-hydroxyformamide potential energy surface

	Relative energy/kcal mol^{-1}	
System[a]	Gas	Solution
1*Z*c	0.0[b]	0.0[c]
1*E*t	4.0	0.5
2*Z*tc	−0.1	5.4
2*Z*tt	0.7	3.9
2*Z*ct	6.4	—
2*E*tc	2.7	7.5
2*E*tt	3.3	7.6
2*E*cc	7.8	10.4
2*E*ct	8.5	10.5
3tc	8.8	9.8
3cc	16.0	13.7
3tt	11.5	8.9
3ct	13.5	14.4
TS1	23.4	25.2
TS2	34.5	46.8
TS3	50.2	62.4
TS4	49.6	64.8
1*Z*-Nanion	328.7	291.2
1*Z*-Oanion	342.9	293.9
1*E*-Oanion	337.6	295.2
2*Z*-Sanion	338.1	292.2
2*E*-Oanion	358.0	315.8
2*E*-Sanion	337.8	365.1

[a] See Scheme 1. [b] ZPVE-corrected energy = −568.070321 hartree. [c] Free energy = −568.133414 hartree.

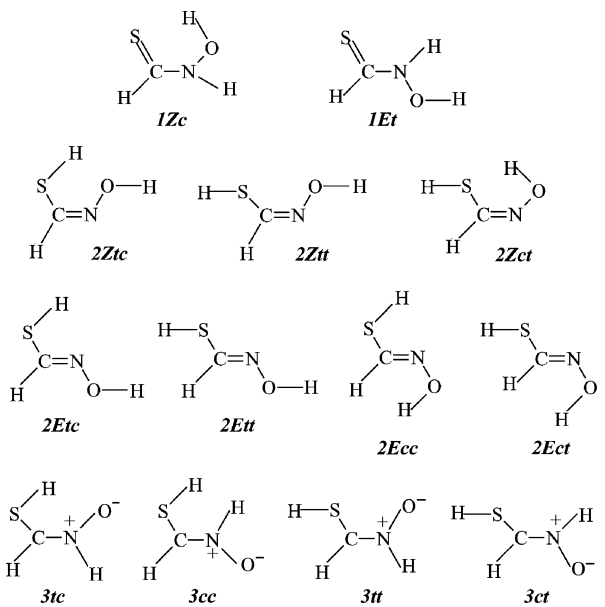

Scheme 1

for formohydroxamic acid,[14] where the two keto forms were found to be definitely preferred over the iminol tautomer.

Both the *Z* forms are stabilized by intramolecular hydrogen bonding. While the hydrogen bond in **1*Z*** is of the S · · · H–O kind, that in **2*Z*** is S–H · · · O. The latter is not possible in hydroxamic acids because of geometric restrictions, as the O–H bond is shorter than the S–H bond. The charge-separated structure **3** is found to be least stable.

It may be noted that many of the structures have energies within 3 kcal mol^{-1} of the global minimum **2*Z***, and so exist in equilibrium in the gas phase at room temperature. Thus **1*Z***, **2*Z*tc** and **2*Z*tt** are present to the extent of 40%, 47% and 12%, respectively, and the thiol forms therefore dominate in the gas phase. Moreover, all these structures have the right orientation for forming chelates with metal ions.

Vibrational frequencies. The stability found for the thiol form, however, does not conform to conclusions based on IR analysis[26] in the solid state, which showed no evidence of the expected S–H stretching band near 2600 cm^{-1}. According to the authors, although it had been earlier reported[27] that weak S–H bands are observed in solutions of thiohydroxamic acids, the bands disappeared on careful purification and recrystallization. It was therefore surmised that the thiohydroximic acid tautomer does not exist. The calculated spectrum for **2*Z***, depicted in Fig. 1, also does not exhibit any band in this region.

Perusal of the computed vibrational frequencies (Table 2) reveals that there is a band at 2598 cm^{-1}, but its intensity is very low and it is dwarfed by the N–O stretching band at 907 cm^{-1}. Thus, the experimental IR spectrum does not rule out the existence of the **2*Z*** tautomer. The small intensity of the S–H band can be understood from a natural population analysis. The calculated partial atomic charges on S and H are −0.005 and 0.170, respectively. Thus the dipole moment and its derivative for this bond are small, and this explains the low intensity of its stretching band. In contrast, the corresponding charge densities on the O and H atoms for the hydroxamic acid analogue are −0.695 and 0.510, respectively, and the O–H stretching band at 3527 cm^{-1} has an intensity of 57 km mol^{-1}. However, the calculated Raman intensity of this band is high, and hence this band should be observable in the Raman spectrum.

The calculated vibrational frequencies are in agreement with the assignment of the experimental infrared spectra for thiohydroxamic acids in carbon tetrachloride solutions.[27] The authors reported the observation of the S–H stretching frequency at ∼2600 cm^{-1}, and three bands in the high frequency region over

Table 2 Calculated vibrational frequencies[a] for the **1*Z*** and **2*Z*** tautomers

1*Z*			**2*Z***		
	Intensity/km mol^{-1}			Intensity/km mol^{-1}	
$\tilde{\nu}$/cm^{-1}	IR	Raman	$\tilde{\nu}$/cm^{-1}	IR	Raman
224	104	1	215	54	4
249	11	3	245	1	3
394	128	4	358	79	4
468	7	0	502	24	0
662	17	5	602	11	3
847	7	1	705	48	5
884	8	17	825	20	2
989	162	0	907	131	9
1235	32	11	944	30	9
1385	77	6	1288	19	10
1422	168	12	1336	90	4
1554	50	8	1623	42	10
3029 (C–H)	15	122	2598 (S–H)	1	74
3230 (O–H)	67	70	3097 (C–H)	5	94
3510 (N–H)	128	138	3617 (O–H)	83	140

[a] Scaled by 0.9614.

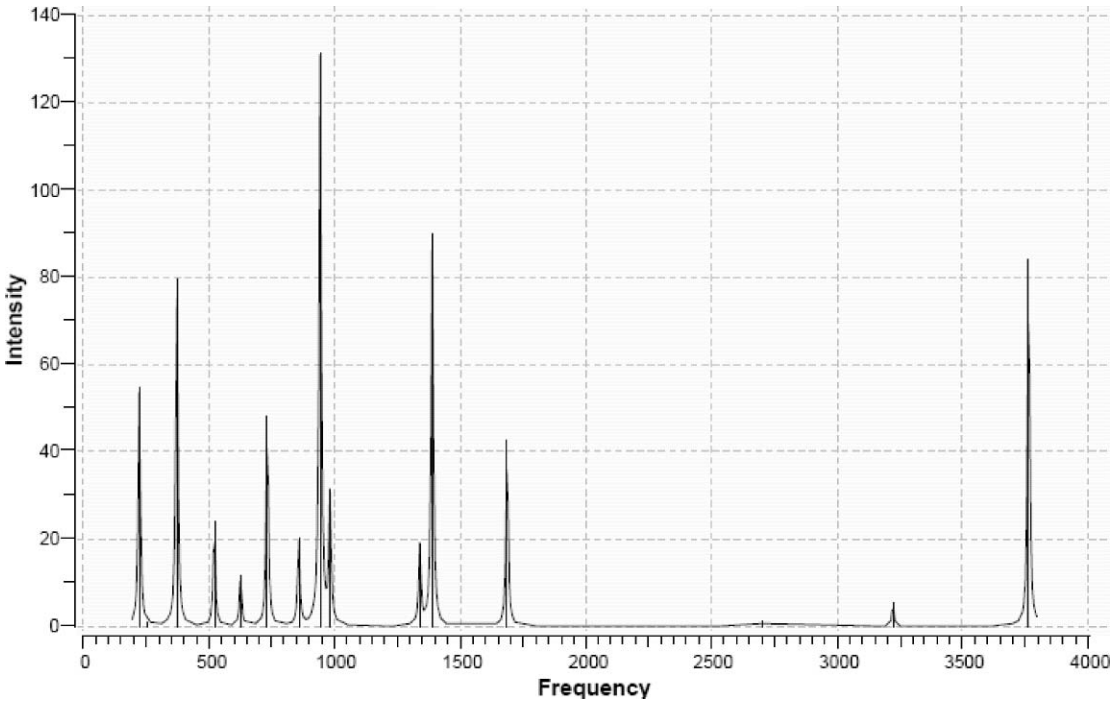

Fig. 1 Computed infrared spectrum of the **2*Z*** tautomer.

3200 cm^{-1}. All the four bands were found to be sensitive to deuteration, suggesting that they all correspond to stretchings of bonds involving hydrogens. These observations can only be reconciled by the presence of both tautomers in solution. The authors assigned a broad band at 3220–3230 cm^{-1} to the associated O–H bond of **1*Z***, while the two non-associated bands at 3580 cm^{-1} and 3405 cm^{-1} were assigned, respectively, to the O–H and N–H bands of **2*Z*** and **1*Z***, in agreement with assignments based on DFT calculations (Table 2). The red shift of the O–H stretching frequency of **1*Z*** and the decrease in its intensity due to hydrogen bonding is clearly apparent from the calculated values given in Table 2. However, the IR spectrum for the solid state does not show the presence of the S–H band,[26,27] indicating that the thione tautomer is stabilized in the solid state by intermolecular association.

Natural bond orbital (NBO) analysis. Table 3 gives an NBO analysis[20] of the **1*Z*** tautomer. The outstanding observation is the transfer of electron density from the nitrogen lone pair to the $C_1{=}S_5$ π^* orbital, resulting in a delocalization of charge in the NCS region. This causes double bond character in the CN bond (the calculated Wiberg[28] bond order is 1.36). The O_4 lone pair also contributes a small amount of electron density to the $C_1{=}S_5$ π^* orbital, decreasing the bond order of this bond to 1.56. The small interaction between H_7 and sulfur (bond order = 0.04) indicates weak hydrogen bonding in this tautomer. This is possibly because of the delocalization in the S–C–N–O bond system, which diverts electron density away from the in-plane sulfur lone pairs.

The previous sections indicated that, in contrast to formohydroxamic acid, the thiol form **2*Z*** is more stable in the gas phase for thioformohydroxamic acid. This difference has been ascribed[13] to the weaker C=S bonding compared to C=O. However, the calculated Wiberg C=S bond order (1.65) is similar to the C=O bond order in the corresponding hydroxamic acid (1.62).

Table 3 NBO analysis of the **1*Z*** tautomer

Energy/eV	Occupancy	Orbital	Centre	%
−0.696	1.99	$n_1(S_5)$	S_5	100
−0.694	1.98	$\sigma(C_1–S_5)$	C_1	58.78
			S_5	41.22
−0.682	1.99	$n_1(O_4)$	O_4	100
−0.574	1.97	$\sigma(C_1–H_3)$	C_1	62.81
			H_3	37.19
−0.346	1.93	$n_2(O_4)$	O_4	100
−0.307	1.59	$n_1(N_2)$	N_2	100
−0.288	2.00	$\pi(C_1–S_5)$	C_1	30.04
			S_5	69.96
−0.208	1.87	$n_2(S_5)$	S_5	100
−0.083	0.47	$\pi^*(C_1–S_5)$	C_1	69.96
			S_5	30.04

The NBO analysis of **2*Z*** is given in Table 4. In this case, the oxygen and sulfur lone pairs donate charge density into the C–N

Table 4 NBO analysis of the **2*Z*** tautomer

Energy/eV	Occupancy	Orbital	Centre	%
−0.685	1.99	$n_1(O_4)$	O_4	100
−0.661	1.99	$\sigma(C_1–S_5)$	C_1	52.39
			S_5	47.61
−0.634	1.99	$n_1(S_5)$	S_5	100
−0.570	1.99	$\sigma(S_5–H_7)$	S_5	58.71
			H_7	41.29
−0.556	1.97	$\sigma(C_1–H_3)$	C_1	62.50
			H_3	37.50
−0.433	1.93	$n_1(N_2)$	N_2	100
−0.346	2.00	$\sigma(C_1–N_2)$	C_1	44.19
			N_2	55.81
−0.326	1.91	$n_2(O_4)$	O_4	100
−0.259	1.86	$n_2(S_5)$	S_5	100
−0.004	0.22	$\pi^*(C_1–N_2)$	C_1	55.81
			N_2	44.19

π* orbital, reducing the C=N bond order to 1.825. There seems to be absence of hydrogen bonding, as the H···O bond order is only 0.01.

Intramolecular proton transfer

We also calculated the potential energy profiles for the reaction paths for intramolecular proton transfer of thioformohydroxamic acid tautomers (see Fig. 2 and 3). The relative energies of the transition states are reported in Table 1. The first reaction considered was the transformation of the stable thione form **1*Z*** to the thiol **2*Z***. This entails the transfer of the O–H proton to sulfur and the N–H proton to oxygen. If the former were to occur first, this would entail the intervention of **3** as an intermediate. However, no transition state for this step could be found. A similar situation was found for pyruvic acid, where the transition state leading to a hydroxyl carbene could not be located[29] because of the absence of any overlap between the migrating proton and the oxygen to which it should migrate to yield the product. Here, as the proton has a greater affinity for oxygen than for sulfur, it prefers to remain closer to the former, weakly bonded to sulfur (bond order = 0.04), as deciphered from the NBO analysis. However, this was not the case for formohydroxamic acid, where the corresponding transformation takes place readily, the activation barrier being only 13.8 kcal mol^{-1}. The difference may also be attributed to the greater delocalization of charge involving the S–C–N–O atom system. This difference is also reflected in the C–N bond distance, which is smaller in the thio compound. Moreover, this proton is only weakly bonded to the oxygen (bond order = 0.71) and its total Wiberg bond index is 0.74. However, the MP2[13] barrier for this transformation has been reported as 9.5 kcal mol^{-1}.

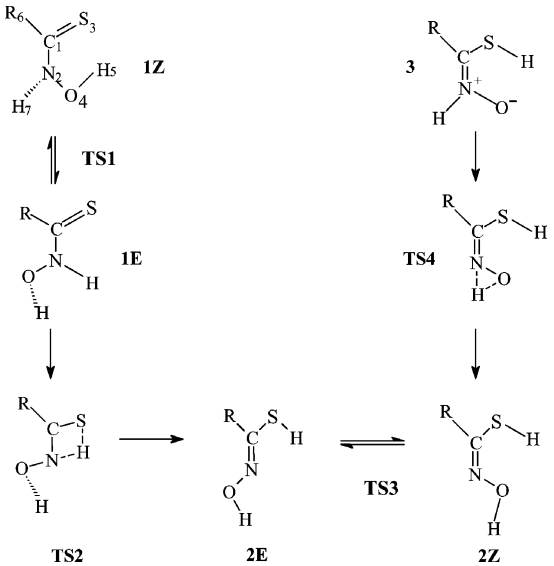

Fig. 2 The tautomeric forms of *N*-hydroxythioamides and the transition states interconnecting them.

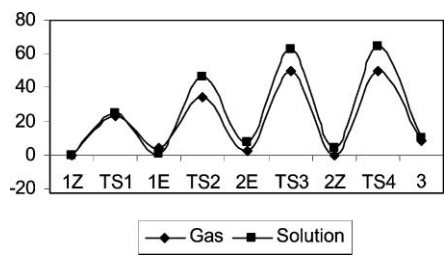

Fig. 3 Schematic potential energy profile for the proton transfer in the gas phase and in aqueous solution.

The transformation of **1*Z*** to **2*E***, therefore, involves first a rotation about the C–N bond leading to **1*E***. This step involves a barrier of 23.4 kcal mol^{-1} *via* **TS1**. This is higher than the general rotational barrier for C–N bonds, which is in the range 10–15 kcal mol^{-1},[30] because of the double bond character of this bond. Transformation of **1*E*** to **2*E*** occurs *via* the transition state **TS2**. This path was found to have an activation energy of 30.5 kcal mol^{-1}. Compared to the case for formohydroxamic acid, there is considerable reduction of the barrier. The MP2[13] barrier is 31.9 kcal mol^{-1}. The authors commented on this decrease in activation barrier and have ascribed it to the release in ring strain due to the larger C–N–H angle in the thio compound. This is found to be so, as there is almost a 10° difference in the calculated bond angles for the hydroxamic acid and the thio analogue, 76.3° and 86.1°, respectively. The interconversion between the thione and thiol form, therefore, occurs *via* a pathway (**1*Z*** → **1*E*** → **2*E*** → **2*Z***) that has an overall activation barrier of 50.2 kcal mol^{-1} (see Fig. 3). The last step involves rotation about the C=N double bond, and is therefore expected to have as large a barrier as that for formohydroxamic acid.[14] The calculated barrier is 47.5 kcal mol^{-1}. In fact, the transition state (**TS3**) has a higher energy (50.2 kcal mol^{-1}) than **TS1** and **TS2**. It is therefore quite likely that the **2*E*** tautomer formed initially (with an activation energy of 34.5 kcal mol^{-1}) does not undergo subsequent isomerization to the more stable rotamer, **2*Z***.

Transformation of **2*Z*** to **3** may, however, occur by the transfer of the O–H proton to nitrogen *via* the transition state **TS4**. This transition state has a high energy because of the presence of a strained three-membered ring (see Fig. 3), and the calculated activation energy for this step is 49.7 kcal mol^{-1}, which is about 9 kcal mol^{-1} higher than that for the corresponding hydroxamic acid. However, there is close agreement between our calculated DFT results and the *ab initio* MP2 value of 51.4 kcal mol^{-1}.

The energy profile is schematically plotted in Fig. 3, from which it is clear that the transition state of highest energy in the path from **1*Z*** to **2*Z*** is **TS3** and is involved in the rate-determining step.

Intermolecular hydrogen bonding

We first performed QM/MM calculations to investigate the effect of aqueous solvation on the relative energies. As stated in the Computational details section, these were performed at the PM3/AMBER level. According to these calculations, the only conformer that gets stabilized on solvation is **1*E***, and this gets stabilized by nearly 30 kcal mol^{-1} with respect to the gas phase. Thus, the thione forms, particularly the *E* conformer, should predominate in solution.

However, calculations with the implicit continuum model PCM (Table 1) show that, although the thione forms again predominate, **1*E*** is slightly less stable than **1*Z***. The total population of the thione forms is 82%, according to the relation $\Delta G = -RT\ln K$. Of this, **1*Z*** is present to the extent of 45%. The thiol forms are present to a total extent of 12%. Although the QM/MM calculations with the QM part treated semiempirically are not expected to be

very accurate, these were performed with nearly 216 explicit water molecules, and are expected to give good indications of the trends of relative stabilities. On the other hand, it has been recognized that the continuum representations are unable to model the dispersion and hydrogen bonding interactions between solute and solvent and the hydrophobic effects of the first few solvation shells.[31]

Since it is not practical to include several solvation shells into a DFT calculation, it seems reasonable to add only a few solvent molecules explicitly and simulate the rest of the solvent by means of a bulk continuum model. Cui[32] used a model in which the solute, glycine, was treated quantum mechanically, the first few solvation shells by MM methods and the rest of the solvent by the PCM continuum model. This approach reproduced the experimentally observed relative stabilities of the neutral and zwitterionic forms of glycine. It has been found that, even with explicit water molecules, the use of a continuum approach for the rest of the solvent system improves results considerably.[33] In the present work, since the PM3/MM calculations showed three water molecules only in the immediate vicinity of the solute, inclusion of more water molecules at the DFT level is computationally too expensive, and it did not improve the calculated enthalpy significantly for the test molecule, **1*E***, we limited our studies to a "solute–solvent cluster" consisting of a supermolecule of thioformohydroxamic acid and three water molecules embedded in a continuum of dielectric 78.39.

The structures that resulted are shown in Scheme 2, where the hydrogen bonds are shown as dotted lines. As stated earlier, these structures were obtained very carefully by a combined QM/MM and molecular dynamics approach. In each case, the same structures resulted even when different orientations of the water molecules in the periodic boxes were taken initially. To validate the selection procedure, other starting geometries were also considered, but they always yielded higher energy structures, sometimes possessing imaginary vibrational frequencies.

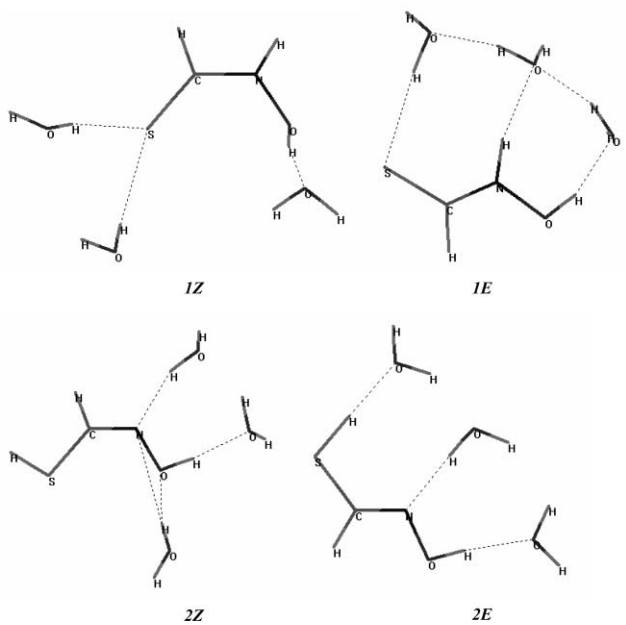

Scheme 2

Table 5 Optimized geometries of **1*Z*** (bond lengths in Ångstroms; bond angles and dihedral angles in degrees) in the gas phase and in solution

Bond parameter[a]	Gas	Solution	Trihydrate	Solvated trihydrate
N_2–C_1	1.328	1.313	1.326	1.319
S_5–C_1	1.667	1.687	1.670	1.680
O_4–N_2	1.380	1.375	1.368	1.371
H_7–O_4	0.993	0.994	1.018	1.019
H_3–C_1	1.091	1.094	1.093	1.091
H_6–N_2	1.010	1.031	1.015	1.016
$S_5C_1N_2$	123.5	125.0	128.6	127.8
$O_4N_2C_1$	122.6	124.9	124.5	123.6
$H_7O_4N_2$	101.6	105.4	105.6	106.0
$H_3C_1N_2$	112.4	111.8	110.4	110.9
$H_6N_2C_1$	126.1	124.1	120.8	123.6
$O_4N_2C_1S_5$	0.0	0.0	−5.2	−5.4
$H_7O_4N_2C_1$	0.0	0.1	90.8	91.0
$H_3C_1N_2O_4$	180.0	180.0	174.6	175.5
$H_6N_2C_1S_5$	180.0	−179.9	−175.2	−176.4

[a] See Fig. 2.

Despite the intramolecular hydrogen bonding in **1*Z***, it is found that it forms a hydrogen-bonded trihydrate. To accommodate the water molecules, large changes in geometry of the substrate molecule occur. In particular, it becomes nonplanar (Table 5). Variations are particularly noticeable in the bond angles, namely, SCN and ONC, which increase by 5.1° and 1.9°, respectively. Consequently, HCN and HNC decrease by 2.0° and 5.3°, respectively. There is also a large increase in the O–H bond distance (+0.025 Å). It was found by geometry optimization that this hydrogen forms a close contact with a water hydrogen (1.60 Å), while sulfur is involved in hydrogen bonding with another water molecule (2.52 Å). Both distances are much smaller than the sum of the van der Waals radii of oxygen and hydrogen (2.60 Å) and sulfur and hydrogen (3.05 Å). There is another water molecule between the two, and this is hydrogen-bonded with the other two water molecules. The respective O···H–O and O···H–S bond angles are found to be 176.7° and 145.1°, showing that the hydroxyl proton forms strong linear hydrogen bonds with water molecules. This weakens the hydroxyl bond. Moreover, the calculated Mulliken charges on the hydroxyl oxygen and hydrogen are −0.526 and 0.457, respectively. The high values of the negative and positive charges also confirm the existence of hydrogen bonding.

The second hydrogen-bonded structure is **1*E***·$3H_2O$. In this case, all the water molecules are hydrogen-bonded to the substrate (Scheme 2). The hydrogen bond distances are 1.83 Å, 1.88 Å and 2.29 Å, respectively, and the O–H···O, N–H···O, and S···H–O bond angles are 158.5°, 159.0° and 171.2°, respectively. Here the sulfur is involved in a linear hydrogen bond. These calculations show that **1*E*** is more strongly hydrated than **1*Z***. In fact, it becomes the more stable rotamer of the thione form, being 4.1 kcal mol^{-1} more stable than the trihydrate of **1*Z***.

All the vibrational frequencies for all trihydrates are found to be real, and this confirms that these are equilibrium structures on the potential energy surface. The relative energies of the trihydrates of **1*E***, **2*Z*tt** and **2*E*tc** are −4.0, −0.4 and 1.7 kcal mol^{-1} with respect to **1*Z***, compared to the corresponding values 4.0, 0.7 and 2.7 kcal mol^{-1} for the gas phase (Table 1). **1*E*** is stabilized to the largest extent and the thione form still remains the most stable.

The preference for the thione forms in aqueous solutions explains why NMR studies could not detect the thiol tautomer.

The energy gap between *Z* and *E* reverses from 4.0 kcal mol^{-1} in the gas phase to −4.1 kcal mol^{-1}, favouring the *E* conformer more than the *Z* structure. A possible reason for this is the fact that stabilization due to the intramolecular hydrogen bonding present in the gas phase is lost due to the formation of intermolecular hydrogen bonds with water molecules in solution. The relative stabilizations of the two conformers can be estimated by comparing their enthalpies of solvation. The enthalpy values were estimated by adding the thermal corrections to the energy to account for translational, vibrational and rotational motion at 298.15 K and atmospheric pressure. The calculated reaction enthalpy for the process

$$\mathbf{1}\boldsymbol{Z} + 3H_2O \rightarrow \mathbf{1}\boldsymbol{Z}\cdot 3H_2O$$

is −31.6 kcal mol^{-1}, and that for

$$\mathbf{1}\boldsymbol{E} + 3H_2O \rightarrow \mathbf{1}\boldsymbol{E}\cdot 3H_2O$$

is −38.9 kcal mol^{-1}. Hence, hydrogen bonding with water stabilizes the higher dipole moment form **1*E*** to a greater extent than it does **1*Z***, which additionally has to undergo a breaking of the previously present intramolecular hydrogen bonding to accommodate the water molecules. This agrees with the general observation that the lower dipole moment conformers are favoured in the gas phase, while the higher dipole moment forms are stabilized in aqueous solution. The trihydrate of **1*E*** is therefore present to the largest extent, and the equilibrium is expected to shift more strongly towards the thione form in aqueous solution.

Aqueous phase calculations

The effect of bulk water was considered by calculating the free energies of the trihydrates of the two rotamers of the thione tautomer in aqueous solution, and it was found that the free energy value for **1*E*** is −6.5 kcal mol^{-1} relative to **1*Z*** at 298.15 K and 1 atmospheric pressure. Thus, the *E* conformer of the thione form becomes more emphatically favoured in aqueous solution. The discrete level calculations had shown that **1*E*** form is stabilized by stronger hydrogen bonding with water molecules than **1*Z***. Thus, bulk solvent calculations alone are not able to model specific hydrogen bonding interactions, unless some explicit water molecules are also included in the calculation.

The variation in the geometries of the **1*Z*** conformer when isolated, complexed with three water molecules and in the bulk water environments is interesting. Table 5 shows that aqueous solvation reduces the C–N bond length by ∼0.009 Å. There is a concomitant increase in the C=S bond length (0.013 Å), signifying that delocalization of electrons takes place from the C=S bond to the C–N bond. However, these changes are smaller than those observed for the formohydroxamic acid analogues.[14] The most important observation is that the explicit solvent model predicts that the hydroxyl hydrogen has to move out of plane to form a strong hydrogen bond with a water molecule, as evidenced by the increase in the O–H bond length. As shown in Fig. 3, in solution, the barrier becomes larger by 12.2 kcal mol^{-1} (see Table 1).

Anions

Three types of anions corresponding to the ionization of a proton from nitrogen, oxygen or sulfur are possible. Since both the **1*Z*** and **2*Z*** forms seem to be favoured in the gas phase, and **1*E*** in aqueous solution, dissociation could occur with either the O–H bond of **1*Z***, making thioformohydroxamic acid an *O*-acid, or with the N–H bond, making it an *N*-acid. In addition, there is a possibility of dissociation from the NO–H group of the equally stable **2*Z***, making thioformohydroxamic acid again an *O*-acid. The S–H proton could also dissociate from **2*Z***. The various possible ions are depicted in Scheme 3.

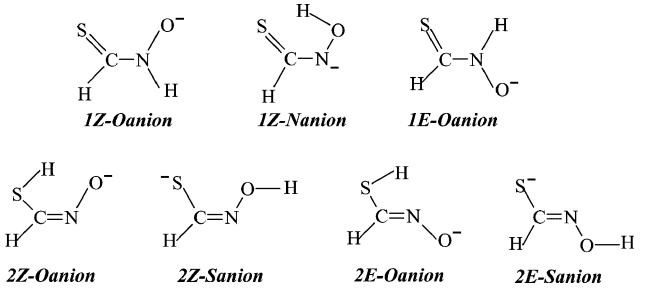

Scheme 3

We have carried out a study of the relative stabilities of the possible anions formed by dissociation of a proton from either the N, O or S atoms, and the results are presented in Table 1. The most stable anion is the *N*-anion formed by deprotonation of **1*Z***. The O–H···S bonding stabilizes this structure. A more appropriate description of this anion is **2*Z*-Sanion**, formed by S–H deprotonation from the **2*Z*ct** rotamer. In contrast, there is no hydrogen bonding possible in the *O*-anion formed from **1*Z***, and this anion is less stable by 14.2 kcal mol^{-1}. Between the *Z* and *E* forms of the *O*-anion, the latter is preferred, as the two electronegative atoms, S and O$^-$, are on opposite sides of the C–N bond and their mutual repulsion is reduced. The *E* form of the *N*-anion is structurally similar to the *S*-anion of **2*Z***, except for the placement of the double bonds. The resultant structure is more similar to the latter, and has been labelled **2*Z*-Sanion**.

The other equally stable tautomer of the undissociated acid is **2*Z***, which may lose an S or an O proton. The latter does not occur for precisely the same reason that **TS1** is not formed. The proton prefers the oxygen, to which it migrates from sulfur on optimization, yielding **1*Z*-Nanion**. The *S*-anion of **2*Z*** is a geometrical isomer of **1*Z*-Nanion** that is 9.4 kcal mol^{-1} higher in energy.

Thus thioformohydroxamic acid may be considered either as an *N*-acid or an *S*-acid, depending on whether one considers proton dissociation from the thione or the thiol tautomer. In the case of formohydroxamic acid, the greater stability of **1*Z*-Nanion** over **1*Z*-Oanion** was explained on the basis of electron resonance involving the N–C=O bonds. The occurrence of resonance in **1*Z*-Nanion** was confirmed by the reduction in the C–N bond length in the anion, and increase in its vibrational frequency. Similarly, the C=O bond length increases and its vibrational frequency reduces. This implies that a resonance exists between the keto and iminol forms, as shown below.

Apparently the N–C=S stabilization is also present in the thio isomer, as the **1*Z*-Nanion** is found to be the most stable. The

Table 6 Calculated change in the partial atomic charges on the various atoms on formation of **1*Z*-Nanion** from **1*Z***, or from **2*Z*** for gaseous thioformohydroxamic acid

Atom[a]	**1*Z*-Nanion**	**1*Z***	Δq_1	**2*Z*ct**	Δq_2
C_1	0.490	0.445	0.045	0.543	−0.053
N_2	−0.471	−0.255	−0.216	−0.401	−0.070
H_3	0.057	0.090	−0.033	0.105	−0.048
O_4	−0.696	−0.658	−0.038	−0.595	−0.101
S_5	−0.830	−0.431	−0.399	−0.233	−0.597
H_6	—	0.350	−0.350	0.113	−0.113
H_7	0.449	0.460	−0.011	0.466	−0.017

[a] All calculations are at the B3LYP/6-311++G(3df,3pd)//B3LYP/6-31G(d) level.

calculated Wiberg C–N and C–S bond orders are 1.73 and 1.24, respectively, compared to 1.61 and 1.36 for the hydroxamic acid analogue. Thus, in this case the equilibrium lies further to the right, the C–S bond being almost a single bond. **1*Z*-Nanion** may therefore also be considered as deprotonated **2*Z*ct**, where the deprotonation occurs from the S–H bond (*S*-acid). From the calculated partial atomic charges on the various atoms in **1*Z***, **2*Z*ct** and **1*Z*-Nanion** (see Table 6), it is also seen that the largest increase in negative charge on formation of the anion occurs at the sulfur. This shows that deprotonation is accompanied by a relocation of electron density, as expected from the tautomeric equilibrium shown in Scheme 4.

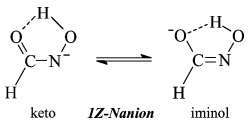

Scheme 4

The calculated proton dissociation free energy for formohydroxamic acid is 322.6 kcal mol^{-1}. This was calculated from the relation $G_{anion} + G_{proton} - G_{1Z}$, where the respective terms are the free energies of **1*Z*-Nanion** (−567.572748 hartree), the proton (−0.01 hartree) and the undissociated **1*Z*** form (−568.096910 hartree), estimated after making the required thermal corrections to the energy arising from the translational, rotational and vibrational motions at 298.15 K and atmospheric pressure. Alternatively, considering ionization from the **2*Z*ct** tautomer ($G = -568.087169$ hartree), the proton dissociation works out to 316.5 kcal mol^{-1}.

In the aqueous phase, too, the PCM calculations show that it is **1*Z*-Nanion** which is most stable (Table 1), but the differences in energy between the various ions are extremely small. As for hydroxamic acids, this anion may exist as a resonance hybrid of the thione and thiol forms. That this occurs can be seen from considerations based on the variation in bond lengths and bond orders (Table 7). Compared to the corresponding values for formohydroxamic acid,[14] these values are very different. In each case, the C–N and O–N bonds are shorter in the thio analogue. The **1*Z*** tautomer gets stabilized in the aqueous phase due to delocalization of charge in the SCN moiety, as evidenced by the decrease in the C–N bond length and increase in the C–S bond length, and consequent changes in the bond orders. Formation of the anion is accompanied by a further increase in the C–N bond order and decrease in the S–C bond order. Solvation of the anion does not have a marked effect on the anion bond lengths or the bond orders.

Table 7 Variation in bond lengths (Å) and bond orders on solvation for the thione form **1*Z*** and the *N*-anion derived from it

Bond	**1*Z***	**1*Z***·3H_2O (aq.)	**1*Z*-Nanion**	**1*Z*-Nanion** (aq.)
Length				
CN	1.327	1.319	1.299	1.295
ON	1.380	1.371	1.412	1.407
SC	1.667	1.680	1.751	1.756
Order				
CN	1.303	1.434	1.727	1.732
ON	1.005	1.019	1.011	1.009
SC	1.654	1.477	1.240	1.228

For aqueous-phase calculations on anions, it is even more important to include explicit water molecules, because these charged species are more highly solvated. In fact, the need for using explicit water molecules arose from the inability of classical continuum models to model amino acids in the zwitterionic form.[32] It has also been shown that, for *N*-acetyl-L-alanine-*N*′-methyl amide (NALANMA), the experimental VA, VCD, Raman, ROA and NMR spectra could only be interpreted if four water molecules were included in the theoretical simulation of the spectra.[34,35] The species that was found to be stable is not even a stable minimum on the gas-phase potential energy surface, but stabilizes on addition of water molecules, indicating that the actual species present is a cluster of NALAMNA with four water molecules.

Because of the very small differences in anion relative stabilities resulting from PCM aqueous-phase calculations, and the fact that inclusion of explicit solvent molecules is likely to have a marked effect on the relative energies, we have repeated the calculations taking a cluster of each anion with water molecules. The same procedure as was used for the tautomers themselves yielded solvated structures having 15 water molecules. It is not computationally feasible to incorporate such a large number of water molecules in a DFT calculation, so we opted for two-layer ONIOM calculations instead, in which the substrate molecule was treated in the same way as in the gas-phase calculations (B3LYP/6-311++G(3df,3pd)//B3LYP/6-31G(d)), but the solvent molecules were treated semiempirically using the PM3 Hamiltonian. This procedure is expected to bring out subtle differences arising from hydrogen bonding and dispersion effects.

For the four anions, **1*Z*-Nanion**, **1*Z*-Oanion**, **1*E*-Oanion** and **2*Z*-Sanion**, the calculated zero-point corrected energies are −567.185676, −567.162897, −567.171632 and −567.153719 hartree, respectively, signifying that the differences in energy are much higher than those predicted from simple PCM calculations alone. Thus, **1*Z*-Nanion** is more stable than the anion that is next highest in stability, **1*E*-Oanion**, by 8.8 kcal mol^{-1}, signifying that thioformohydroxamic acid is decisively a nitrogen acid in aqueous solution.

N-Hydroxythioacetamide and *N*-methyl-*N*-thioformylohydroxylamine

The next higher homologue of *N*-hydroxythioformamide is *N*-hydroxythioacetamide (thioacetohydroxamic acid), and its *N*-methyl substituted isomer is *N*-methyl-*N*-thioformylohydroxylamine (*N*-methylthioformohydroxamic acid), commonly known

Table 8 DFT relative energies (kcal mol^{-1}) of the various stationary points on the gas-phase thioacetohydroxamic acid and *N*-methylthioformohydroxamic acid potential energy surfaces

System	Thioacetohydroxamic acid	*N*-Methylthioformohydroxamic acid
1*Z*	0.0[a]	5.0
1*E*	4.7	10.4
2*Z*	0.1	—
2*E*	3.1	—
TS3	50.8	—
1*Z*-Oanion	345.7	350.5
1*E*-Oanion	340.6	345.3
1*Z*-Nanion	330.2	—
2*Z*-Sanion	340.6	—
2*E*-Oanion	360.1	—

[a] ZPVE-corrected energy = −607.378610 hartree.

as thioformin. The latter may exist only in the thione form, and is less stable than its *C*-methyl isomer by 5.0 kcal mol^{-1} (see Table 8). As for thioformohydroxamic acid, both the thione and thiol forms are equally stable for thioacetohydroxamic acid. Unlike hydroxamic acids, the energy gap between the **1*E*** and **1*Z*** forms becomes larger with substitution (see Table 8).

As far as the activation barriers are concerned, since for thioformohydroxamic acid the pathway from **1*Z*** to **2*Z*** must depend on **TS3**, we have calculated the energy of only this transition state. For the gas phase, the overall barriers are 50.2 and 50.8 kcal mol^{-1}, respectively, for thioformo- and thioacetohydroxamic acids. The barriers between the thione and thiol forms thus remain almost unchanged upon methyl substitution. This is expected, since the reaction coordinate involves motion of mainly the nitrogen and hydroxyl hydrogen.

The relative energies of the anions are also given in Table 8. The observation that **1*Z*-Nanion** is the most stable signifies that the higher homologue is also essentially an *N*-acid in the gas phase. Our calculated value for the proton dissociation free energy of thioacetohydroxamic acid is 324.3 kcal mol^{-1}.

In contrast to the situation for thioformo- and thioacetohydroxamic acids, in *N*-substituted derivatives there is no possibility of the thiol form, as the nitrogen lacks a hydrogen atom for transfer to the carbonyl oxygen. For the anion, it is found that the *O*-anion formed from **1*E*** is more stable than that from **1*Z*** by 5.2 kcal mol^{-1} (see Table 8). This is because of the repulsion between the negatively charged electronegative atoms, S and O, on the same side in the latter. The calculated proton dissociation energy is 334.1 kcal mol^{-1}.

Discussion

We conclude the paper with a short discussion about the calculation methodology and possible sources of error. The first point concerns the choice of exchange functional. Today a plethora of exchange functionals exist, and it often becomes difficult to judge which is applicable to a particular system. Current applications of DFT are based on its local density approximation (LDA) generalized gradient (GGA) functionals, which in the field of molecular calculations have been progressively abandoned in favour of more accurate recent developments, such as meta-GGA[36,37] and hybrid functionals,[38] or newer empirical versions of GGA functionals.[39]

Of the hybrid functionals, B3LYP is the most widely used, as it reproduces geometries and energies of small molecules very well. Despite its proven successes, it is now becoming apparent that it sometimes fails to accurately describe the energies of van der Waals molecules and hydrogen-bonded systems. Reaction barrier heights and large molecules are also inadequately represented.[40–43] In a recent comparison of various functionals in reproducing stabilization energies of n-alkanes,[44] it was deduced that two GGA functionals, PW91[45] and the "parameter-free" PBE,[46] performed better than B3LYP, and described the binding in attractive van der Waals regions more accurately. These functionals are also attractive, particularly for solids, as they avoid calculating the nonlocal exact exchange, and are hence computationally less expensive. However, PW91 has a tendency to avoid non-classical structures and transition states, as observed in the case of carbenes.[47] In another work,[48] we had carried out a comparison of various LDA and GGA functionals for describing the geometries of Cu(II) hydroxamate complexes, and found the PBE functional to be the most reliable. However, in general, while the LDA functionals suffer from a tendency to overbind atoms, GGA functionals correct this tendency but underbind instead. For example, in the case of rare gas dimers, PW91 and PBE exchange-only potentials lead to erratic minima.[49]

For the sake of comparison, a few calculations, for which MP2[13] results are available, were repeated with the PBE functional. Though both MP2 and B3LYP predict the **2*Z*** tautomer of thioformohydroxamic acid to be more stable than **1*Z***, PBE incorrectly predicts that **1*Z*** should be more stable by 1.6 kcal mol^{-1}. This reinforces our contention that LDA and GGA results should be treated with caution. However, the PBE-calculated activation barrier for the transformation (50.2 kcal mol^{-1}) agrees with the values calculated at the MP2[13] (51.4 kcal mol^{-1}) and B3LYP (50.2 kcal mol^{-1}) levels.

The main differences in the various DFT methods lie in the treatment of dynamic electron correlation, which is completely neglected in the Hartree–Fock approximation. Most well-established density functionals, including B3LYP, use local electron densities and do not account for medium-[50] and long-range dispersion interactions.[51] Moreover, local exchange functionals also suffer from other defects, one of these being that they take into account a spurious interaction of an electron with itself, the "self-exchange" problem.

One finds that at present there is no one functional that is universally applicable to molecules, solids and other systems, and that describes all situations very well. The design of such functionals is the focus of much current research. The recent hybrid meta-GGAs[36,37] are a step in this direction, but are not adequately tested as yet. Another alternative to the exact nonlocal exchange is the optimized effective potential (OEP) method, which generates local exchange functionals for atoms. The OEP method has been recently extended[52] by the Bartlett group to generate local OEP correlation functionals based on MP2 correlation energies and potentials, and this method has been termed *ab initio* DFT by the authors.

It may also be added that, when one considers larger molecules, such as biomolecules, the choice of calculation method becomes even more crucial. Not only is there a need to keep computational

Table 9 Calculated heats of formation (kcal mol^{-1}) of the various points on the gas phase thioformohydroxamic acid potential energy surface

System	AM1	PM3	PM6
1*Z*	13.2	26.2	11.1
1*E*	15.9	28.6	14.7
2*Z*	−1.8	8.7	0.3
2*E*	−1.0	7.4	2.5
3	15.6	13.6	9.8

costs down, but at the same time accuracy should not be lost. Several efforts are being made to improve the accuracy and reliability of semiempirical methods. The PM3 method of Stewart[22] has been a popular method for the semiempirical treatment of large molecules. We had earlier[53] compared the two semiempirical methods, AM1[54] and PM3, for hydroxamic acids, and had concluded that the former has a slight edge over PM3, as it predicts the correct order of stabilities and geometries of the tautomers and anions, when compared with *ab initio* and DFT results. Recently, Stewart has released an improved version of PM3 to correct its faults and limitations. The new version, PM6, is available in MOPAC 7.2.‡ According to the author, the hydrogen bond and other weak bonds are represented more accurately in PM6. Average errors in geometry and ΔH_f are reduced. Other successes include the correct prediction that acetylacetone is more stable as the enol form than the dione, and that anthroquinone is planar. The incidence of wildly incorrect results is also claimed to be reduced. However, the program is still in its beta version and is under development. There are still some faults that may be corrected by more parameterization, but some are unlikely to be corrected.

At this stage of its development, it is useful to compare results from PM6 with those from other methods. Table 9 compares the heats of formation obtained by the various semiempirical methods. Immediately one notices that the calculated heats of formation, which were calculated too high by the PM3 method, are comparable to the AM1 values now. However, even after this improvement, the stabilities of the thiol forms and the charge-separated form, **3**, are too highly exaggerated when compared with the DFT and MP2[13] energy values. However, the **1*Z***–**1*E*** enthalpy difference (3.6 kcal mol^{-1}) is now closer to the DFT energy difference (4.0 kcal mol^{-1}), suggesting that hydrogen bonding is better accounted for by PM6.

Efforts are also being made to extend the range of DFT methods to larger systems through approximations. One approximate DFT method is the self-consistent charge density functional tight-binding (SCC-DFTB) scheme,[55,56] which has been shown to be able to give a reliable description of reaction energies, geometries, and vibrational properties of small organic molecules. The SCC-DFTB scheme has been combined with the AMBER force field, so that the hybrid SCC-DFTB/MM method can be applied to larger biological systems that *ab initio* QM/MM cannot handle.[57] Test calculations, performed for the water dimer, H_2CO–H_2O, NH_3–H_2O, formamide–H_2O, NMA–H_2O, and AAMA + 4H_2O complexes, showed that, for most of the test systems, the correct order of relative energies was obtained, as compared with the *ab initio* calculations. However, the SCC-DFTB method somewhat underestimates the hydrogen bonding energies as compared with the higher level DFT (B3LYP) calculations.[56]

One may hope that soon there will be a DFT functional that best describes all kinds of systems, from molecules to solids, from strongly bonded to weakly bonded, and which gives accurate values for a large number of properties at less computational expense than conventional G3 calculations. Until such functionals are tested, B3LYP remains the method of choice for small molecules, such as those studied here. B3LYP is good for almost any property when applied to small molecules, but yields to less "popular" functionals as molecules increase in size.[58] For example, B3LYP achieves a high accuracy (mean absolute deviation (MAD) = 0.13 eV) for thermochemistry, *i.e.*, heats of formation of the 148 molecules in the extended G2 reference set.[59,60]

In view of the proven ability of the hybrid functional B3LYP to accurately reproduce geometries and energies of small molecules, we have used it in the present calculations. Wherever possible, we have compared our results with those from MP2 calculations,[13] and found satisfactory agreement, both for relative stabilities and for activation barriers. For instance, B3LYP, along with other DFT functionals, does not treat charge-transfer effects correctly in excited-state calculations. Doubts have therefore been expressed against the use of this functional for describing bond-breaking and bond-making processes. The excellent agreement with MP2 results of activation barriers for this system indicates that B3LYP is able to satisfactorily reproduce barriers for such processes at a fraction of the computational cost of MP2 calculations.

Conclusions and perspectives

Our calculations on the various systems related to thiohydroxamic acids reveal that both the thione (**1**) and thiol (**2**) tautomers are equally stable in the gas phase, but in aqueous solution, the thione tautomer is favoured. The presence of both tautomers is in agreement with experimental infrared studies. However, infrared spectroscopy may fail to distinguish between the two tautomers, because of the small intensity of the S–H stretching band, but Raman spectroscopy may reveal this band. The barrier to the interconversion between these two forms is of the order of 50 kcal mol^{-1}, but this increases in aqueous solution. The barrier to the rotation of **2*E*** to the more stable rotamer, **2*Z***, is significant, and this affects the activation energy for the transformation of **1*Z*** to **2*Z***. It is unequivocally proved that proton dissociation occurs from the nitrogen atom, making these *N*-acids. It is also found that the proton dissociation free energies decrease with methyl substitution. However, for the *N*-methyl derivative, the proton dissociation energy is higher, because this is an *O*-acid.

To model the interactions in the aqueous phase, it is very important that a few explicit water molecules be included in the calculation, particularly for charged species, as implicit solvent calculations are unable to accurately describe the geometrical and other changes that result from specific hydrogen-bonding interactions.

Although the present calculations represent a fairly detailed investigation of *N*-hydroxythioamides, there is scope for further work. As discussed above, the results are dependent on several interrelated factors, some of these being the choice of calculation method, including how the correlation and exchange energies are treated (functional), and how the solvent is modelled. In this case

‡ http://openmopac.net/

in particular, where the several species have similar energies, the relative energies are expected to be very sensitive to these factors.

In comparisons with experimental quantities, the effects of dynamics and temperature, as well as solvent polarity, need to be considered, too. We have found that the relative stabilities and activation energies change drastically from the gas phase to solution. Further, since these acids play a biological role, the dielectric constant of the environment is expected to have a profound effect, as the molecular forces that dictate and control the affinities and the specificities of biological interactions are modulated by the microenvironments in which they are expressed. In future work, we aim to address these issues.

References

1 A. Chimiak, W. Przychodzen and J. Rachon, *Heteroat. Chem.*, 2002, **13**, 169–194.
2 W. Walter and E. Schaumann, *Synthesis*, 1971, **3**, 111–130, and references cited therein.
3 A. J. Mitchell, K. S. Murray, P. J. Newman and P. E. Clark, *Aust. J. Chem.*, 1977, **30**, 2439–2453.
4 D. H. R. Barton and R. A. V. Embse, *Tetrahedron*, 1998, **54**, 12475.
5 G. Winkelmann, D. van der Helm and J. B. Neilands, *Iron Transport in Microbes, Plants and Animals*, VCH, Weinheim/New York, 1987.
6 Y. Egawa, K. Umino, Y. Ito and T. Okuda, *J. Antibiot.*, 1971, **24**, 124–130.
7 S. Itoh, K. Inuzuka and T. Suzuki, *J. Antibiot.*, 1970, **23**, 542–545.
8 K. Shirahata, T. Deguchi, T. Hayashi, I. Matsubara and T. Suzuki, *J. Antibiot.*, 1970, **23**, 546–550.
9 T. Miyagashima, T. Yamaguchi and K. Umino, *Chem. Pharm. Bull.*, 1974, **22**, 2283–2287.
10 T. Miyagashima, *Chem. Pharm. Bull.*, 1974, **22**, 2288–2293.
11 K. Nagata and S. Mizukami, *Chem. Pharm. Bull.*, 1966, **14**, 1263–1272.
12 B. S. Sekhon, *Indian J. Chem.*, 1994, **33A**, 237–238.
13 S.-J. Yen and J.-J. Ho, *J. Phys. Chem. A*, 2000, **104**, 8551–8557.
14 R. Kakkar, R. Grover and P. Chadha, *Org. Biomol. Chem.*, 2003, **1**, 2200–2206.
15 A. D. Becke, *Phys. Rev. A*, 1988, **38**, 3098–3100.
16 C. Lee, W. Yang and R. G. Parr, *Phys. Rev. B: Condens. Matter*, 1988, **37**, 785–789.
17 S. H. Vosko, L. Wilk and M. Nusair, *Can. J. Phys.*, 1980, **58**, 1200–1211.
18 M. J. Frisch, G. W. Trucks, H. B. Schlegel, G. E. Scuseria, M. A. Robb, J. R. Cheeseman, J. A. Montgomery, Jr., T. Vreven, K. N. Kudin, J. C. Burant, J. M. Millam, S. S. Iyengar, J. Tomasi, V. Barone, B. Mennucci, M. Cossi, G. Scalmani, N. Rega, G. A. Petersson, H. Nakatsuji, M. Hada, M. Ehara, K. Toyota, R. Fukuda, J. Hasegawa, M. Ishida, T. Nakajima, Y. Honda, O. Kitao, H. Nakai, M. Klene, X. Li, J. E. Knox, H. P. Hratchian, J. B. Cross, C. Adamo, J. Jaramillo, R. Gomperts, R. E. Stratmann, O. Yazyev, A. J. Austin, R. Cammi, C. Pomelli, J. W. Ochterski, P. Y. Ayala, K. Morokuma, G. A. Voth, P. Salvador, J. J. Dannenberg, V. G. Zakrzewski, S. Dapprich, A. D. Daniels, M. C. Strain, O. Farkas, D. K. Malick, A. D. Rabuck, K. Raghavachari, J. B. Foresman, J. V. Ortiz, Q. Cui, A. G. Baboul, S. Clifford, J. Cioslowski, B. B. Stefanov, G. Liu, A. Liashenko, P. Piskorz, I. Komaromi, R. L. Martin, D. J. Fox, T. Keith, M. A. Al-Laham, C. Y. Peng, A. Nanayakkara, M. Challacombe, P. M. W. Gill, B. Johnson, W. Chen, M. W. Wong, C. Gonzalez and J. A. Pople, *GAUSSIAN 03 (Revision B.5)*, Gaussian, Inc., Wallingford, CT, 2003.
19 A. P. Scott and L. Radom, *J. Phys. Chem.*, 1996, **100**, 16502–16513.
20 E. D. Glendening, A. E. Reed, J. E. Carpenter and F. Weinhold, *NBO Version 3.1*, Theoretical Chemistry Institute, University of Wisconsin, Madison, 2003.
21 W. L. Jorgensen, J. Chandrasekhar, J. D. Madura, R. W. Impey and M. L. Klein, *J. Chem. Phys.*, 1983, **79**, 926–935.
22 J. J. P. Stewart, *J. Comput. Chem.*, 1989, **10**, 209–220; J. J. P. Stewart, *J. Comput. Chem.*, 1989, **10**, 221–264.
23 W. D. Cornell, P. Cieplak, C. I. Bayly, I. R. Gould, K. M. Merz, Jr., D. M. Ferguson, D. C. Spellmeyer, T. Fox, J. W. Caldwell and P. A. Kollman, *J. Am. Chem. Soc.*, 1995, **117**, 5179–5197.
24 Hypercube, Inc., Florida Science and Technology Park, 1115 NW 4th Street, Gainesville, FL 32601; http://www.hyper.com/.
25 M. Cossi, G. Scalmani, N. Rega and V. Barone, *J. Chem. Phys.*, 2002, **117**, 43–54.
26 K. A. Jensen, O. Buchardt and C. Christophersen, *Acta Chem. Scand.*, 1967, **21**, 1936–1941.
27 K. Nagata and S. Mizukami, *Chem. Pharm. Bull.*, 1966, **14**, 1255–1262.
28 K. B. Wiberg, *Tetrahedron*, 1968, **24**, 1083–1096.
29 R. Kakkar, M. Pathak and N. P. Radhika, *Org. Biomol. Chem.*, 2006, **4**, 886–895.
30 C. E. Blom and Hs. H. Günthard, *Chem. Phys. Lett.*, 1981, **84**, 267–271.
31 C. J. Cramer and D. G. Truhlar, *Chem. Rev.*, 1999, **99**, 2161–2200.
32 Q. Cui, *J. Chem. Phys.*, 2002, **117**, 4720–4728.
33 V. W. Jürgensen and K. Jalkanen, *Phys. Biol.*, 2006, **3**, S63–S79.
34 W. G. Han, K. J. Jalkanen and S. Suhai, *J. Phys. Chem. B*, 1998, **102**, 2587–2602.
35 K. J. Jalkanen and S. Suhai, *Chem. Phys.*, 1996, **208**, 81–116.
36 J. P. Perdew, S. Kurth, A. Zupan and P. Blaha, *Phys. Rev. Lett.*, 1999, **82**, 2544–2547.
37 T. Van Voorhis and G. E. Scuseria, *J. Chem. Phys.*, 1998, **109**, 400–410.
38 A. D. Becke, *J. Chem. Phys.*, 1993, **98**, 1372–1377; A. D. Becke, *J. Chem. Phys.*, 1993, **98**, 5648–5652.
39 F. A. Hamprecht, A. J. Cohen, D. J. Tozer and N. C. Handy, *J. Chem. Phys.*, 1998, **109**, 6264–6271.
40 B. J. Lynch, P. I. Fast, M. Harris and D. G. Truhlar, *J. Phys. Chem. A*, 2000, **104**, 4811–4815.
41 Y. Zhao, O. Tishchenko and D.G. Truhlar, *J. Phys. Chem. B*, 2005, **109**, 19046–19051.
42 S. Tsuzuki and H. P. Luthi, *J. Chem. Phys.*, 2001, **114**, 3949–3957.
43 J. A. Duncan and M. C. Spong, *J. Phys. Org. Chem.*, 2005, **18**, 462–467.
44 M. D. Wodrich, C. Corminboeuf and P. v. R. Schleyer, *Org. Lett.*, 2006, **8**, 3631–3634.
45 J. P. Perdew, in *Electronic Structure in Solids '91*, ed. P. Ziesche and H. Eschrig, Akademie Verlag, Berlin, 1991, p. 11.
46 J. P. Perdew, K. Burke and M. Ernzerhof, *Phys. Rev. Lett.*, 1996, **77**, 3865–3868.
47 R. Kakkar, R. Garg and P. Chadha, *THEOCHEM*, 2002, **617**, 143–149.
48 R. Kakkar, R. Grover and P. Gahlot, *Polyhedron*, 2006, **25**, 759–766.
49 X. Xu and W. A. Goddard, III, *Proc. Natl. Acad. Sci. U. S. A.*, 2004, **101**, 2673–2677.
50 S. Grimme, *Angew. Chem., Int. Ed.*, 2006, **45**, 625–629 and references cited therein.
51 W. Koch and M. C. Holthausen, *A Chemist's Guide to Density Functional Theory* (2nd edn), Wiley-VCH, Weinheim, 2001, p. 236.
52 S. Hirata, S. Ivanov, I. Grabowski, R. J. Bartlett, K. Burke and J. D. Talman, *J. Chem. Phys.*, 2001, **115**, 1635–1649.
53 R. Kakkar, P. Grover and P. Chadha, *Org. Biomol. Chem.*, 2003, **1**, 2200–2206.
54 M. J. S. Dewar, E. G. Zoebisch, E. F. Healy and J. J. P. Stewart, *J. Am. Chem. Soc.*, 1985, **107**, 3902–3909; M. J. S. Dewar and Y. C. Yuan, *Inorg. Chem.*, 1990, **29**, 3881–3890.
55 M. Elstner, D. Porezag, G. Jungnickel, J. Elsner, M. Haugk, Th. Frauenheim, S. Suhai and G. Seifert, *Phys. Rev. B*, 1998, **58**, 7260–7268.
56 M. Elstner, D. Porezag, G. Jungnickel, Th. Frauenheim, S. Suhai and G. Seifert, in *Tight Binding Approach to Computational Materials Science*, ed. P. Turchi, A. Gonis and A. Colombo, *MRS Symp. Proc. No. 491* (Materials Research Society), Pittsburgh, PA, 1998.
57 W.-G. Han, M. Elstner, K. J. Jalkanen, T. Frauenheim and S. Suhai, *Int. J. Quantum Chem.*, 2000, **78**, 459–479.
58 V. N. Staroverov, G. E. Scuseria, J. Tao and J. P. Perdew, *J. Chem. Phys.*, 2003, **119**, 12129–12137.
59 L. A. Curtiss, K. Raghavachari, G. W. Trucks and J. A. Pople, *J. Chem. Phys.*, 1991, **94**, 7221–7230.
60 L. A. Curtiss, K. Raghavachari, P. C. Redfern and J. A. Pople, *J. Chem. Phys.*, 1997, **106**, 1063–1079.